9th ANKARA INTERNATIONAL AEROSPACE CONFERENCE **AIAC-2017-086**
20-22 September 2017 - METU, Ankara TURKEY

IMPLEMENTATION OF THE SUBMODELLING TECHNIQUE ON THE DOVETAIL ATTACHMENTS

Ahmet Arda Akay*, Demirkan Çöker†, Altan Kayran‡ and Ercan Gürses§
Middle East Technical University
Ankara, Turkey

ABSTRACT

In this study, a critical component of an aeroengine compressor disc which is called dovetail attachment is numerically investigated. A dovetail attachment consists of two main components: the blade and the disc. During the operation of the engine, highly stressed areas occur at the interface of the disc and the blade. Peak values of these stressed areas are mainly localized at the edges of the contact area between the disc and the blade. These stresses are non-singular and can converge to a finite value with successive mesh refinement. For this purpose, a submodelling procedure is introduced which can provide an accurate solution without the requirement of very high computational efforts. The submodelling is implemented for the finite element analysis of the dovetail attachment and convergence of the peak stresses is demonstrated.

INTRODUCTION

Aeroengine compressor discs mainly consist of three critical components: the hub region, the dovetail-rim region and the areas that contain assembly holes or welds [Meguid et al., 1996]. During the flight of the air vehicle, centrifugal forces of the blades, loads generated by spacers and assembly bolts and thermal stresses act on the components of the aeroengine. Due to these loads, highly stressed areas occur in the components of the engine [Papanikos et al., 1998]. In order to prevent a catastrophic failure of the compressor disc, it is vital to have a sustainable engine design regarding to these loads on the components.

In this study, dovetail-rim region of an aeroengine compressor disc under the action of the centrifugal forces of the blades is investigated. A detailed dovetail-rim region of an aeroengine for a single blade section is given in Figure 1. During the operation of the engine, the blades are rotating at a high speed which causes a radially outward movement of the blades. Due to the centrifugal forces, the dovetail root-blade presses against the dovetail slot-disc which prevents the radial motion of the blade assembly. Accordingly, highly stressed areas occur at the interface of the disc and the blade. Fretting fatigue phenomenon is commonly seen in these attachments, which results in premature failure due to

*GRA in Department of Aerospace Engineering, Email: aakay@metu.edu.tr
†Assoc. Prof. in Department of Aerospace Engineering, Email: coker@metu.edu.tr
‡Prof. in Department of Aerospace Engineering, Email: akayran@metu.edu.tr
§Assoc. Prof. in Department of Aerospace Engineering, Email: gurses@metu.edu.tr

cracking or wear. Main cause of the fretting fatigue is high stress gradients occuring near the edges of contact. In [Sinclair et al., 2002], these stresses are proved to be nonsingular and converges to a finite value with successive mesh refinement on the edges of contact. To obtain reliable elastic stresses by using modest computing resources, submodelling approach introduced in [Cormier et al., 1999] is implemented to the finite element analyses. Submodelling can be briefly explained as cutting out a region of interest and modelling it separately. Boundary conditions of the extracted submodel are taken from a previously solved global model. The submodelling technique allows the analyst to have a solution with high resolution in a region of interest without the requirement of high computational resource.

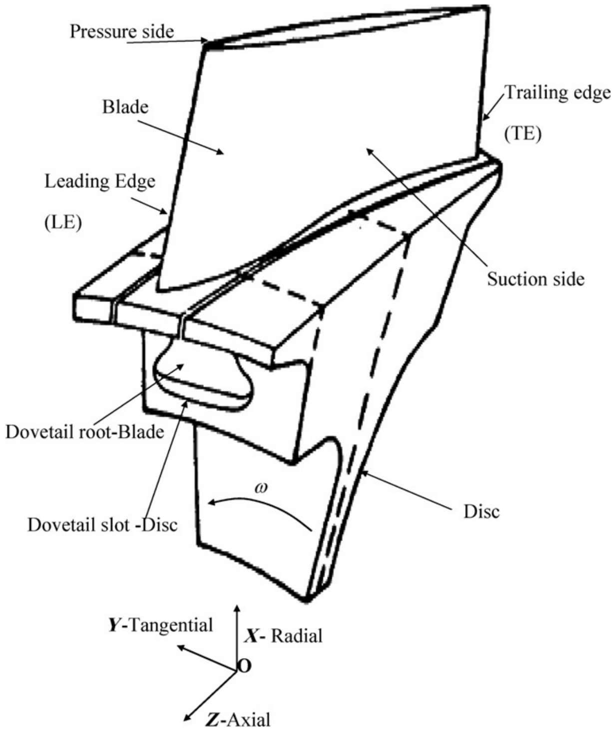

Figure 1: Bladed-disc rotor section of a typical aeroengine compressor disc [Anandavel and Prakash, 2011]

METHOD

The first application of the submodelling method to the finite element analysis of the dovetail specimen is presented by [Cormier et al., 1999]. Some of the early applications of the submodelling approach on different geometries are cited therein. The difference of this work from the former submodelling applications is that it has a ratio of global model area to submodel area around 200 to 1, whereas the maximum value of the ratio was 50 to 1 in previous papers. In [Cormier et al., 1999], the submodelling technique is firstly used on an engineering problem which has an exact analytic solution. After verifying the analytical solution with the submodel results, it is implemented on a 2D dovetail geometry and the convergence of the peak contact stress is demonstrated. [Cormier et al., 1999] use displacement shape functions as boundary condition on the boundaries of the submodel. [Sinclair and Epps, 2002] state that the use of displacement shape functions may yield to logarithmic stress singularities on the the submodel boundary. Instead, cubic splines may be fit to the boundaries of the submodel and they can be used as the boundary condition [Sinclair and Epps, 2002]. Stress values at the edges of contact for dovetail geometry are proved to be converging to a value with successive mesh refinement of the submodel, see [Sinclair et al., 2002]. Hence, these stresses appears to be non-singular since they have a convergence behaviour. Accordingly, numerical verification of non-singular stress state for dovetail attachment is presented in [Sinclair et al., 2002]. The first application of the submodelling approach on 3D dovetail finite element model is done by [Beisheim and Sinclair, 2003]. The convergence of the peak stress on 3D model is observed; however, the contact between the disc and the blade is assumed to be frictionless in this study. The most extensive dovetail analyses are conducted in [Anandavel and Prakash, 2011]. 3D finite element analyses are done for 15 different loading conditions including angular velocity and aero-dynamical loads. Hence, effects of the skew angle of the dovetail on the results are presented. It is deducted that for a 3D straight dovetail model, the variation of peak stress in the thickness direction is negligible.

The procedure of the implementation of submodelling used in this work is extensively discussed in [Akay, 2016]. It can briefly be described as cutting out a critical section of a global model and modelling it separately by taking its boundary conditions from previously solved coarser global model. Extracted boundary conditions are applied to the boundaries of the subtracted submodel. A linear interpolation is used to determine the displacement values of the intervening nodes on the submodels. The difference of this work from the previous studies is that in each sub-step of analysis the extracted values of the displacements and the displacements of the intervening nodes determined by linear interpolation are applied to the boundary nodes of the submodel. The reason for submodelling operation is quite obvious. To have a converged sought-after stress, one needs to have a mesh fine enough in the critical region so that the stress will no longer be dependent on the mesh size. However, following such a procedure on a global model will not be computationally efficient. Hence, because of the complexity of the superfine global model, it may not usually possible to have a converged solution with a limited computational resource.

Geometry and Finite Element Model

The geometric model presented in [Papanikos et al., 1998] is used for the two dimensional submodelling study on the dovetail joint. Geometric details and dimensions of the blade and the disc geometries are given in Figure 2a. Investigated geometry is a single part of the cyclic sector of rotor. Moreover, due to the symmetry of the single dovetail section, finite element model of the half section is created as shown in Figure 2b. Material properties of the Ti-alloy used for dovetail joint are provided in Table 1. Material is assumed to have isotropic and linear elastic behaviour.

A cylindrical coordinate system is defined to the center of the circular disc part of the dovetail joint. The finite element model is shown in Figure 2b. Due to the symmetry condition of the model, displacements of the nodes on the edges highlighted with orange color (letter A) are constraint in θ-direction. Hence, in order to prevent the rigid body motion, displacements of the nodes on the edges highlighted with red color (letter C) are constraint in r-direction. Analyses are carried out in one load step with 10 sub-steps. An angular velocity of 1050 rad/s is applied at the center of circular disc as shown with purple color in Figure 2b [Anandavel and Prakash, 2011]. The blade is subjected to the angular velocity. Due to the angular velocity, a steady centrifugal force is acting at center of gravity of the blade.

Frictional contact with a friction coefficient of 0.3 is defined between the disc and the blade bodies. 3-node line-to-line contact is defined between contacting bodies. The disc and the blade bodies are defined as the target and the contact bodies, respectively. ANSYS TARGE169 and CONTA172 elements are used for the modelling of the target and the contact surfaces, respectively. For the contact enforcement method, the Normal Lagrange method is used.

Table 1: Material properties of aero-engine [Anandavel and Prakash, 2011]

Elastic Modulus [GPa]	Poisson's Ratio [-]	Density [kg/m^3]
110	0.30	4500

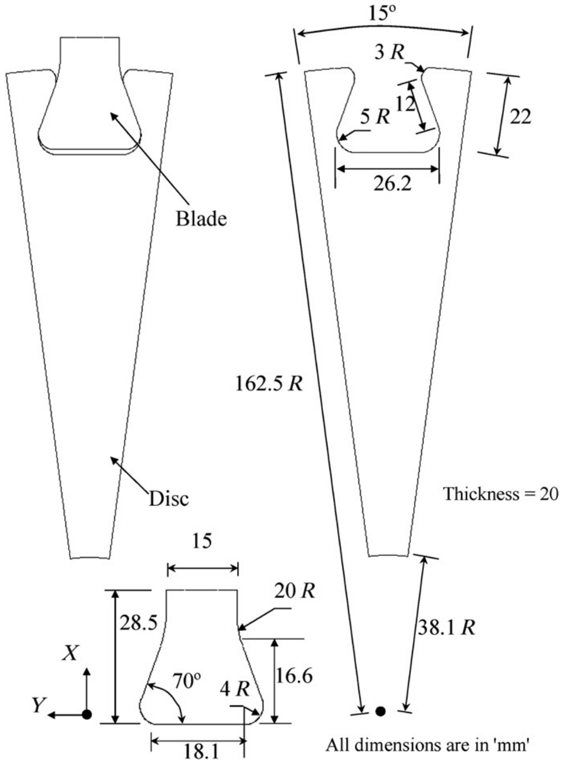

(a) Geometric details of dovetail joint (dimensions are in millimetres)[Papanikos et al., 1998]

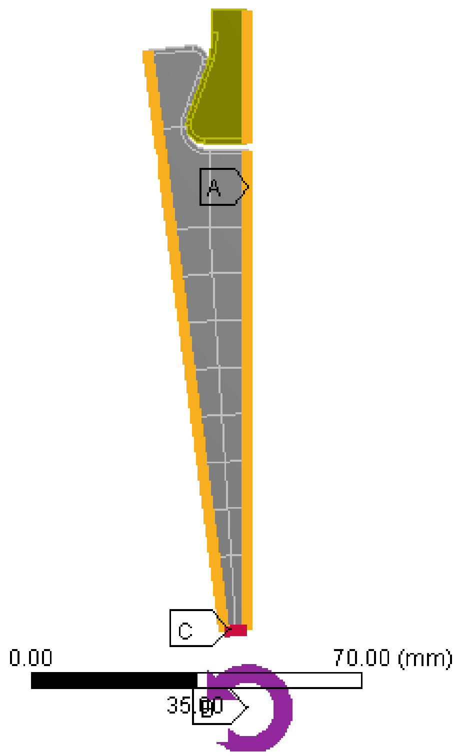

(b) Loadings and boundary conditions for the finite element model

Figure 2: Geometric features and finite element model of the dovetail joint

Meshing and Submodels

First, a preliminary finite element analysis of the global model with the defined loading is performed. It is seen that for the dovetail geometry, the maximum equivalent stress occurs at the bottom edge of the contact, so the submodel will be selected in the neighbourhood of that location. To adjust the meshing properties, a boundary layer, which includes the critical region that is going to be investigated through submodelling, should be defined. In [Cormier et al., 1999], it is stated that a ratio of 4 between the thickness of the boundary layer and the smaller local radius of curvature R is adequate. The smaller local radius of curvature for this model is 3 mm, so the thickness of the boundary layer should have a value around 0.75 mm. Boundary layer is highlighted in Figure 3a.

To have systematic mesh couples (coarse, medium, fine) on global model, edge sizing is defined on certain edges. These edges are highlighted in Figure 3. The edge sizing parameters regarding to the mesh of boundary layer, which are highlighted in Figure 3a, are successively halved between the coarse and the medium global models and between the medium and the fine global models. The element sizing is given to the straight edges of the boundary layer. For the arcs within the boundary layer, line division is set according to the outer length of the arc. Given division is calculated by the ratio between outer arc length and element sizing given to the straight edges of the boundary layer. All surfaces regarding to the boundary layer is set to mapped face meshing to have uniform mesh inside it. Outside of the boundary layer, to the edges highlighted in Figure 3b, edge divisions are given. The change is done in a systematic way. Each mesh parameter share a common ratio at the transition between meshes. There is no need to successively halve mesh size outside of the boundary layer, since its effect on the edge of contact stress is negligible. They are regarded as the transition elements.

For the dovetail analysis, selected submodel is presented in Figure 4. Before proceeding to submodelling, three global models with mesh sizes coarse (C), medium (M) and fine (F) are created. To see the convergence behaviour of the maximum stress value, convergence check given in Equation 1a may be used. Superscripts C, M and F used in below equation denote the maximum stress values

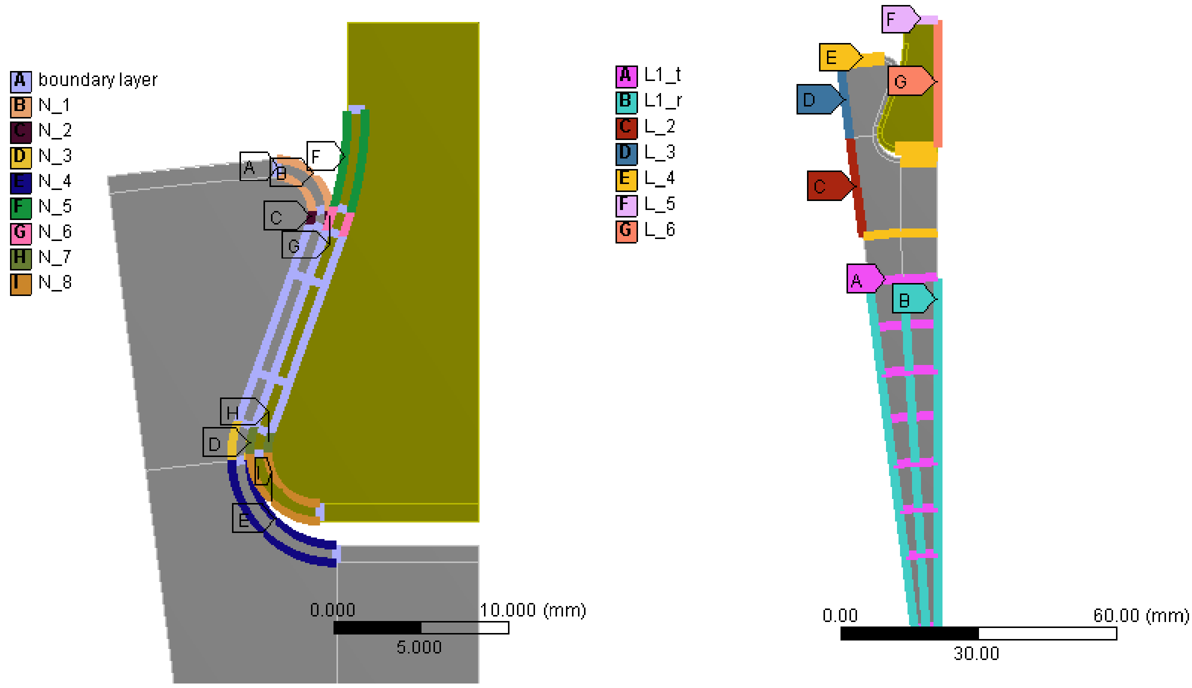

(a) Inside of the boundary layer

(b) Outside of the boundary layer

Figure 3: Edges that are defined with a sizing value to have a systematic mesh

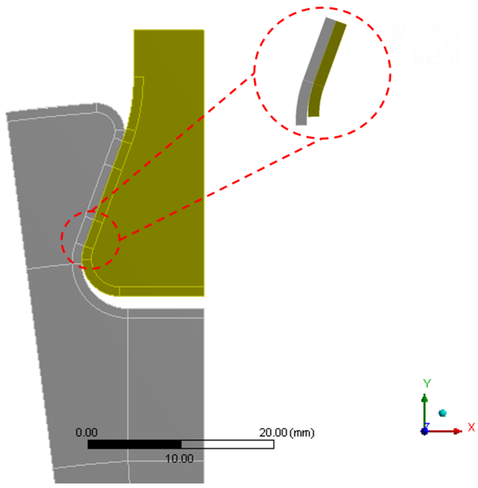

Figure 4: Submodel

corresponding to the coarse, the medium and the fine grids, respectively. If no convergence is seen, a superfine global grid may be created and convergence check may be done between the medium, the fine and the superfine grids. However, such an operation would not be reasonable in terms of computational effort. To check whether or not the peak stress has converged, a second convergence check given in Equation 1b may be used. $\epsilon_s = 0.01$ is considered as excellent accuracy, $\epsilon_s = 0.05$ as good, $\epsilon_s = 0.1$ as satisfactory and $\epsilon_s > 0.1$ as unsatisfactory [Beisheim and Sinclair, 2003]. If the ϵ_s value is in desired limits for the global models, there will be no need for a submodel and convergence is achieved. Otherwise, submodelling is necessary to have convergence. In Table 2, it is seen that the convergence of the peak stress is not observed for the global models. Error value is way beyond the desired limits. Therefore, submodelling is necessary to converge the peak stress.

$$|\sigma^M_{max} - \sigma^C_{max}| > |\sigma^M_{max} - \sigma^F_{max}| \tag{1a}$$

$$|\frac{\sigma^F_{max} - \sigma^M_{max}}{\sigma^F_{max}}| < \epsilon_s \tag{1b}$$

Table 2: Maximum equivalent stress for coarse, medium, fine global models and their convergence checks

Stress Component	Coarse Mesh [MPa]	Medium Mesh [MPa]	Fine Mesh [MPa]
σ_{eqv}	131.76	169	209.19
Convergence Check According to Equation 1a		**Error Value ϵ According to Equation 1b**	
Not satisfied		0.19	

RESULTS

A coordinate system is defined on bodies as shown in Figure 5. Stress results are presented according to the defined coordinate system. On the coordinate system, x and y directions defined as parallel and perpendicular directions to the contact line, respectively. In Tables 3 and 4, the maximum peak stress values on the disc and the blade are presented, respectively. Hence, the error values defined in Equations 1a and 1b are calculated for each stress component. They are calculated between the medium and the fine meshes of each global and submodel results. By individually comparing each stress component with the global model and the submodel results, it is seen that after the implementation of the submodelling approach, the stress results are converged in desired limits.

(a) On the disc (b) On the blade

Figure 5: The paths defined for the stress output (shown in red)

Table 3: Maximum normal and shear stresses at the edge of contact on the disc for both global and submodels with their errors

Models	Peak Stress Components	Coarse [MPa]	Medium [MPa]	Fine [MPa]	Error, ϵ [-]
Global	$\sigma_{x,max}$	106.77	120.42	136.28	0.12
	$\sigma_{y,max}$	109.64	151.47	179.71	0.16
	$\tau_{xy,max}$	30.34	34.54	45.91	0.25
Submodel	$\sigma_{x,max}$	149.08	163.65	172.25	0.05
	$\sigma_{y,max}$	202.76	223.90	224.67	0.0034
	$\tau_{xy,max}$	53.67	61.37	63.66	0.036

Table 4: Maximum normal and shear stresses at the edge of contact on the blade for both global and submodels with their errors

Models	Peak Stress Components	Coarse [MPa]	Medium [MPa]	Fine [MPa]	Error, ϵ [-]
Global	$\sigma_{x,max}$	108.62	151.43	201.06	0.25
	$\sigma_{y,max}$	103.93	150.25	174.74	0.14
	$\tau_{xy,max}$	31.76	41.72	49.58	0.15
Submodel	$\sigma_{x,max}$	228.39	246.57	252.73	0.024
	$\sigma_{y,max}$	211.82	224.89	225.13	0.001
	$\tau_{xy,max}$	56.40	61.64	64.79	0.049

In Figure 6, the peak contact stress result on the defined path is visualized. Convergence of the peak stresses with submodelling can be observed in the zoomed view on peak locations, see Figure 6b. Furthermore, in order to compare the accuracy of the submodel, two more global models are created with smaller mesh sizes compared to fine global model. These models are called as the superfine (S) and the extra-superfine (ES) global models. This approach is not always possible due to limits of computational resources, however, it is possible for our model problem to ensure the correctness of the submodelling approach. The results of these models are presented in Figure 7. It is seen that two curves of the different models are almost on top of each other. Solution times of the global models and the submodels are presented in Table 5. It is observed that the fine submodel has the accuracy close to the extra-superfine global model with a eight-nine times quicker solution time.

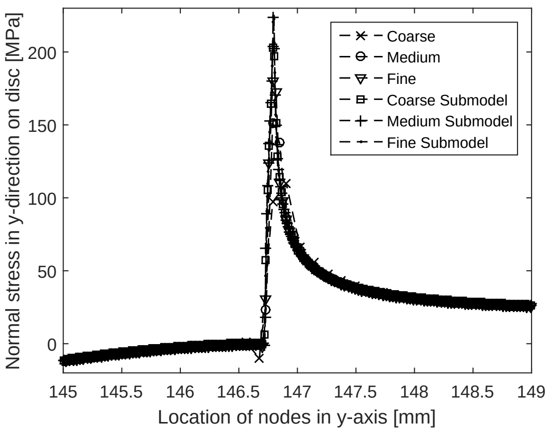

(a) General view

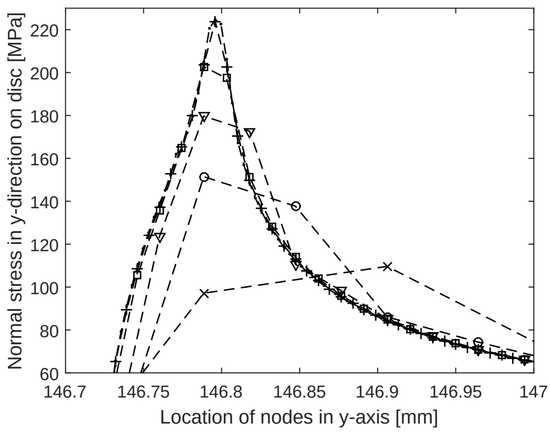

(b) Zoomed view on the peak location

Figure 6: Normal stress in y-direction σ_y on the disc for three global and three submodels on the defined path

Table 5: Solution times of the global models and the submodels

	Solution Time [s]				
Models	**Coarse**	**Medium**	**Fine**	**Superfine**	**Extra-superfine**
Global Model	20.0	60.8	229.0	840.3	6664.6
Submodel	48.7	197.5	800.5	N/A	N/A

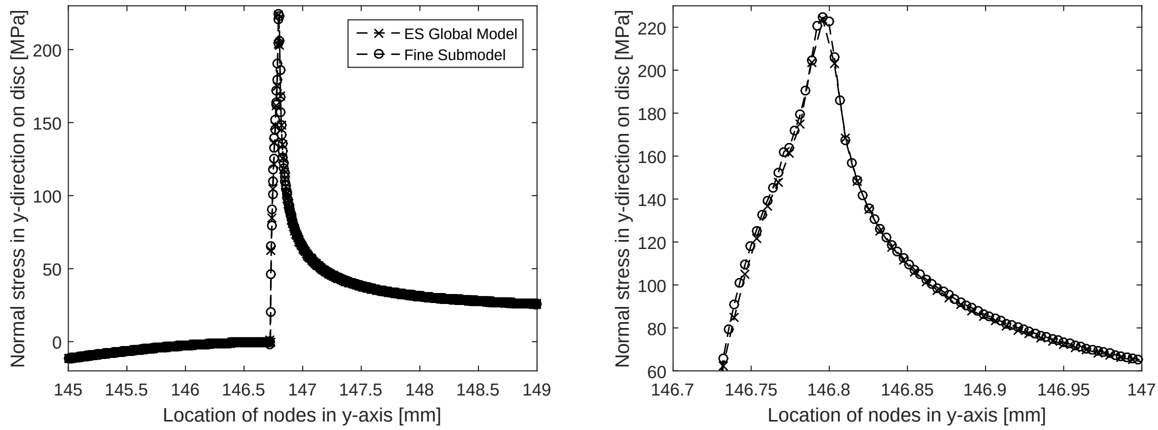

(a) General view (b) Zoomed view on the peak location

Figure 7: Normal stress in y-direction σ_y on disc for extra-superfine global model and fine submodel on the defined path

The loadings and the boundary conditions of the dovetail model are taken from [Anandavel and Prakash, 2011]. To validate the results obtained by submodelling, the converged contact stress results in the article are presented in Figure 8. In the article, a 3D dovetail model is solved. In the figure, the axis shown with "x/a" defines the contact line between the disc and the blade, and the axis shown with "y/a" represents the axis perpendicular to the contact (the thickness direction of submodel). The stress peak located at x/a = -0.1 is the location of the peak stress that is converged in this study. In the figure, it is seen that the maximum converged contact stress has an approximate value of 210-220 MPa, which is consistent with the contact stress results (σ_y) obtained with the submodelling given in the Tables 3 and 4.

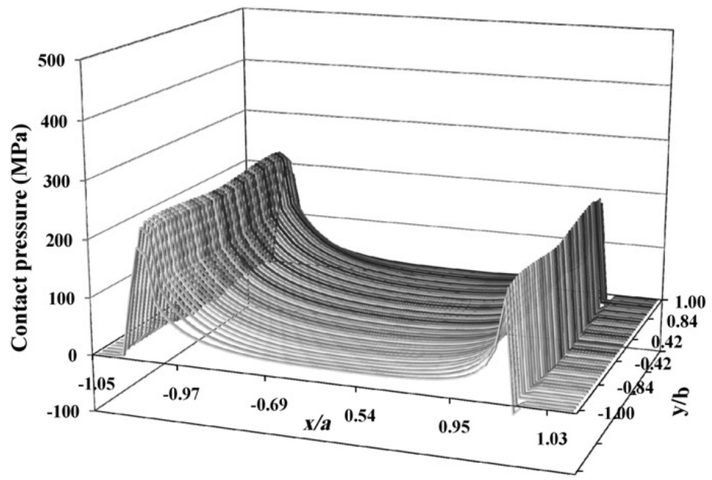

Figure 8: Contact stress distribution between the disc and the blade [Anandavel and Prakash, 2011]

CONCLUSION

Dovetail joints are widely used real aeroengine compressor disc components. A dovetail consists of two parts; the blade and the disc. Due to the rotation of the engine shaft, centrifugal forces acts on the blade which give an radial outward motion to the blade part. However, this movement is constrained with the disc part and high stresses occur at contact surface between the blade and the disc. At the edges of the contact, these stresses have their peak values. Determination of the true contact stresses at these locations are crucial, since the crack initiations generally occur at these locations. It is seen that the bottom edge of the contact is the most critical section and the submodelling technique is implemented to this region. Convergence of the peak contact stresses are observed in the submodels. To compare the accuracy of the submodel, global models having a similar mesh size to the medium and fine submodels at the region of interest are created. These models are called as superfine and extra-superfine global models. It is seen that fine submodel yield the same result with the corresponding extra-superfine global model with a significantly less computational time. The solution with submodelling technique is about eight/nine times faster compared to global model solution with the same accuracy.

ACKNOWLEDGEMENT

I would like to thank to the thesis program of the Turkish Ministry of Science, Industry and Technology (SANTEZ) for their financial support on the project that I have been involved for three years with project code of 055.STZ.2013-1.

References

Ahmet Arda Akay. Finite element analysis and experimental study of dovetail attachments. Master's thesis, Middle East Technical University, 2016.

K Anandavel and Raghu V Prakash. Effect of three-dimensional loading on macroscopic fretting aspects of an aero-engine blade–disc dovetail interface. *Tribology International*, 44(11):1544–1555, 2011.

JR Beisheim and GB Sinclair. On the three-dimensional finite element analysis of dovetail attachments. *Journal of Turbomachinery*, 125(2):372–379, 2003.

NG Cormier, BS Smallwood, GB Sinclair, and G Meda. Aggressive submodelling of stress concentrations. *International Journal for Numerical Methods in Engineering*, 46(6):889–909, 1999.

SA Meguid, MH Refaat, and P Papanikos. Theoretical and experimental studies of structural integrity of dovetail joints in aeroengine discs. *Journal of Materials Processing Technology*, 56(1):668–677, 1996.

P Papanikos, SA Meguid, and Z Stjepanovic. Three-dimensional nonlinear finite element analysis of dovetail joints in aeroengine discs. *Finite Elements in Analysis and Design*, 29(3):173–186, 1998.

GB Sinclair and BP Epps. On the logarithmic stress singularities induced by the use of displacement shape functions in boundary conditions in submodelling. *Communications in Numerical Methods in Engineering*, 18(2):121–130, 2002.

GB Sinclair, NG Cormier, JH Griffin, and G Meda. Contact stresses in dovetail attachments: finite element modeling. *Journal of Engineering for Gas Turbines and Power*, 124(1):182–189, 2002.